# FUNCTIONAL BIOREACTOR CHARACTERIZATION TO ASSESS POTENTIALS OF NANOCOMPOSITES BASED ON DIFFERENT ALGINATE TYPES AND SILVER NANOPARTICLES FOR USE AS CARTILAGE TISSUE IMPLANTS

Jovana Zvicer, Vesna Miskovic-Stankovic, Bojana Obradovic

Faculty of Technology and Metallurgy, University of Belgrade, Belgrade, Serbia

Short title: **Functional bioreactor characterization of biomaterials with respect to application**

Corresponding author:

B. Obradovic

Faculty of Technology and Metallurgy, University of Belgrade

Karnegijeva 4

11000 Belgrade

Serbia

Tel: +381-11-3370414

Fax: +381-11-3370387

E-mail: bojana@tmf.bg.ac.rs



This article has been accepted for publication and undergone full peer review but has not been through the copyediting, typesetting, pagination and proofreading process, which may lead to differences between this version and the Version of Record. Please cite this article as doi: 10.1002/jbm.a.36590

**ABSTRACT**

In this work, functional characterization of biomaterials concerning potential application as articular cartilage implants was performed by using a biomimetic bioreactor with dynamic compression in the physiological regime (10 % strain, 0.84 Hz frequency, 1 h on/1 h off). Specifically, two alginate types with low (*LG*) and high (*HG*) guluronic/mannuronic residue ratios with electrochemically synthesized silver nanoparticles (AgNPs) were evaluated. *HG* Ag/alginate hydrogels were clearly indicated as potential candidates due to better initial mechanical properties as compared to *LG* hydrogels (dynamic compression modulus of ~60 vs. ~40 kPa) as well as the mechanical stability displayed during 7 days of dynamic compression. Cytotoxicity studies in 3D bovine cartilage explant cultures under dynamic compression have shown negligible effects as compared to standard 2D monolayers of bovine chondrocytes where moderate cytotoxicity was observed. Finally, experimental and mathematical modeling studies revealed different mechanisms of AgNP release under physiological-like bioreactor conditions as compared to static conditions. Overall, the results clearly demonstrate bioreactor advantages in characterization and selection of candidate biomaterials as well as potentials to bridge the *in vitro-in vivo* gap.

**Keywords**: 3D systems; cytotoxicity; biomimetic bioreactor; alginate types; silver nanoparticles

## INTRODUCTION

Development of novel biomaterials aimed for biomedical applications requires comprehensive biomaterial characterization and evaluation regarding physico-chemical properties, cytotoxicity, genotoxicity, biocompatibility, long-term stability, and functionality.[1-4] Characterization of nanomaterials and nanocomposites is further complicated due to potential nanotoxicity and nanoparticle accumulation in the body and environment, thus requiring detailed analyses of possible release routes and fate of nanoparticles.

Cytotoxicity of biomaterials is routinely determined in *in vitro* studies in 2D monolayer cell cultures followed by *in vivo* studies in animals. *In vitro* studies are performed as a direct contact test, in which the cells are directly exposed to the investigated material, and the elution test, in which the cells are exposed to the material extract. These tests are carried out over short periods of time (3 hours to 4 days) and thus are time- and cost efficient, allowing rapid evaluation by standardized protocols at high throughputs and providing quantitative and comparable results.[5] However, extrapolation of the obtained outcomes to the *in vivo* settings could be misleading due to drawbacks of the 2D environment, thus creating the *in vitro – in vivo* gap.[6,7] In specific, cells in monolayer cultures are depolarized and lose their specific phenotype due to decreased cell-cell interactions and loss of the extracellular matrix (ECM).[6,8]*In vivo* studies, on the contrary, allow evaluation of long-term effects and functionality of biomaterials, and, in the case of nanoparticles, tissue localization, biodistribution, and retention or excretion from the body.[9] However, these studies are burdened with complexity of the physiological environment, ethical considerations, high costs and practical limitations so that the need for more physiologically relevant *in vitro* 3D culture systems has been recognized.[10] Advances in

that direction have been made in cancer and drug screening research, by using 3D spheroids and cell aggregates, which allow maintenance of the cell phenotype, physiological cell density, and production of ECM components.[8,11,12] In addition to providing 3D structure, culture conditions should also mimic the *in vivo* environment in respect to mass transport (i.e. efficient delivery of chemical signals and removal of metabolites), hydrodynamic environment and physical cues. For example, laminar flow of the culture medium was shown to be a more realistic setting as compared to static cell cultures owing to continuous nutrient supply, steady state regime, physiological shear stresses and improved nanoparticle distribution.[6] Biomimetic bioreactors that imitate native physiological environment are recognized as valuable tools for characterization of novel biomaterials and cell-biomaterial interactions regarding potential applications (e.g. [13,14]). In specific, two important uses of these bioreactors can be distinguished. The first is to provide functional characterization of novel biomaterials over longer times to predict biomaterial behavior after implantation, such as mechanical stability, degradation rates, and release kinetics of active components. The second is in cytotoxicity studies by instituting relevant *in vitro* settings in 3D tissue cultures under physiological conditions, therefore addressing the *in vitro-in vivo* gap.

We have previously developed Ag/alginate nanocomposites with electrochemically synthesized silver nanoparticles (AgNPs) for biomedical applications.[15,16] Alginate is a natural polysaccharide that easily forms biocompatible and hydrophilic hydrogels with high sorption capacity. However, alginate as a natural product derived from brown seaweed differs in composition, molecular weight and physical properties depending on the algae species and age, the harvesting season, and ecological system (geographical origin).[17-19] More homogeneous

alginate composition is obtained by biosynthesis using two genera of bacteria (*Pseudomonas* and *Azotobacter*), but still some variations and different material properties could appear.[20,21] In specific, the content and arrangement of guluronic (G) and mannuronic (M) acid residues influence Na-alginate solution viscosity as well as mechanical and swelling properties of resulting Ca-alginate hydrogels so that alginates with higher G contents generally yield stronger hydrogels.[14,22] Variations in alginate composition are recognized in industry as a problem that is solved from a batch to batch.[23] This issue is even more pronounced in pharmaceutical and medical applications in which the product properties have to be strictly controlled and precisely defined. Consequently, different alginates will be suitable for different purposes and it is of the utmost importance to define key features needed for a particular application early in the product development.

In the present work, we have evaluated the hypothesis that biomimetic bioreactors could be used for functional biomaterial characterization identifying potentials for particular applications, specifically as cartilage tissue implants. Two types of alginate were used with the aim to evaluate the influence of alginate properties on AgNP synthesis and resulting hydrogel characteristics. A biomimetic bioreactor with dynamic compression in the physiological regime relevant for articular cartilage was utilized to functionally evaluate the obtained Ag/alginate nanocomposites regarding biomechanical stability, cytotoxicity and silver release kinetics.

## MATERIALS AND METHODS

### Materials

Two types of sodium alginate with different compositions were used. Low viscosity sodium alginate (A3249, AppliChem, Darmstadt, Germany) was reported to have a high content of

guluronic (G) residues resulting in the M/G ratio of 1.38.[24] Fractions of MM and GG dimmers were estimated as 0.26 and 0.41, respectively.[24] This alginate type was denoted here as high G – *HG*. Medium viscosity sodium alginate (A2033, Sigma, St. Louis, MO), was reported to have lower content of G residues and the M/G ratio of 1.94, as well as a higher fraction of MM dimmers (0.47) as compared to GG blocks (0.16).[24] This alginate type was denoted here as low G – *LG*. Polyvinyl alcohol (PVA, hot water soluble, P163-250G), polyvinylpyrrolidone (PVP, Mw = 40,000) sodium citrate dehydrate and proline were all supplied from Sigma (St. Louis, MO). $AgNO_3$ was purchased from M. P. Hemija (Belgrade, Serbia), $KNO_3$, $Ca(NO_3)_2$ x $4H_2O$ and NaCl from Centrohem (Stara Pazova, Serbia), HCl (37 % v/v) and $HNO_3$ (65 % wt) from ZorkaPharma (Sabac, Serbia), $NH_4OH$ (25 % wt) from NRK Inzenjering (Belgrade, Serbia) and collagenase type II from Gibco Life Technology (Grand Island, NY). Dulbecco's Modified Eagle Medium with 4.5 g/l glucose and 0.584 g/l L-glutamine (DMEM, 01-055-1), 2-[4-(2-hydroxyethyl)piperazin-1-yl]ethanesulfonic acid (HEPES), fetal bovine serum (FBS), penicillin and streptomycin were obtained from Biological Industries (Beit-Haemek, Israel), while ascorbic acid was bought from Galenika (Belgrade, Serbia). Water from Milli-Q system (Millipore, Billerica, MA) was used in all experiments and $N_2$ gas was of high purity (99.5 %). Copper plates (>99.9 %, Cooper mill, Sevojno) and silicone sealant (Bison, Netherlands) were purchased in a local store.

**Electrochemical synthesis of silver nanoparticles**

AgNPs were electrochemically synthesized in 2 % w/v sodium alginate solutions containing 0.1 M $KNO_3$ and 3.9 mM $AgNO_3$, as described previously[15,16,25]and briefly explained in the Supplementary material. Three batches of colloid solutions were synthesized using the low viscosity *HG* sodium alginate and three batches using the medium viscosity *LG* sodium alginate.

**Production of Ag/alginate discs**

Both types of heat-treated Ag/alginate colloid solutions, *HG* and *LG*, were used to produce Ag/alginate discs by pouring 20 ml of the colloid into a sterile Petri dish between two filter papers saturated in 3 % w/v solution of $Ca(NO_3)_2$ x 4 $H_2O$, which served as a gelling agent. Additional 20 - 30 ml of the gelling solution was then slowly poured over the upper filter paper and the dishes were left for 24 h. After this period, discs (12 mm in diameter x 2 mm thick) were cored out of the obtained hydrogels and left for another 24 h in 30 ml of the fresh gelling solution to complete gelation.

**Production of PVA/PVP discs**

PVA/PVP discs were produced by dissolving PVA and PVP powders in hot water at concentrations of 17 and 10 % w/v, respectively, and gelled as described in detail in the Supplementary material. After gelation, discs (12 mm in diameter x 2 mm thick) were cored out and left in 30 ml of the fresh culture medium until the use. The culture medium contained DMEM, supplemented with 10 % FBS, 10 mM HEPES, 100 U/ml penicillin, 100 µg/ml streptomycin, 0.4 mM proline, and 50 µg/ml ascorbic acid and was used in all experiments.

**Isolation of articular cartilage explants and chondrocytes**

Articular cartilage was harvested aseptically from femoropatellar grooves of 4 week old bovine calves within 8 hours of slaughter. Explants (discs 12 mm in diameter and 2 mm thick) and chondrocytes used for cytotoxicity studies were obtained by procedures described previously[27] and briefly summarized in the Supplementary material.

**Bioreactor with dynamic compression**

Functional characterization and cytotoxicity studies of Ag/alginate discs were performed in the bioreactor with dynamic compression described previously[28] and in the Supplementary material. In each experimental series, three cartridges were simultaneously loaded and each was connected to a separate recirculation loop consisting of a medium reservoir, silicone tubing, and an extra tubing coil serving as a gas exchanger. Each loop was filled with 15 ml of the appropriate medium, if it is not stated differently, and the bioreactor system was placed in a humidified 5 % $CO_2$ incubator at 37$^{o}$C and continuously recirculated by a multichannel peristaltic pump at the medium flowrate of 0.12 ml/min. In all experiments, dynamic uniaxial unconfined compression was performed in the regime 1 h on/1 h off, at the loading rate of 337.5 µm/s, 0.84 Hz frequency, and 0.2 mm total displacement corresponding to approximately 10 % strain of the Ag/alginate disc. The compression parameters were selected based on cartilage tissue engineering studies reported in literature (e.g. [29-32]) and our previous studies of alginate based hydrogels.[14,26,33,34]

**Stability of Ag/alginate discs under bioreactor conditions**

Both *HG* and *LG* discs (n=3) were evaluated regarding stability and mechanical properties in the culture medium in the bioreactor for up to 7 days. Outputs from the bioreactor load sensor were acquired daily and applied stresses were calculated by using the plunger area as described previously.[14] The obtained values were then smoothed by a 5-point centered moving average filter and dynamic compression moduli were calculated from the slopes of the best linear fits of resulting stress-strain curves.

**Cytotoxicity studies**

*HG* Ag/alginate discs were investigated regarding cytotoxicity in monolayer chondrocyte cultures (2D) and in the biomimetic bioreactor in cartilage explant cultures (3D).

Monolayer cell cultures

Four experimental groups for cytotoxicity evaluation in 2D were established in 6 well culture plates with: D1 - *HG* Ag/alginate discs, D2 -copper plates as a reference toxic material as suggested in literature[35,36], D3 - silicone sealant as a reference biocompatible material, and D4 - the control monolayer culture group. Ag/alginate discs were fixed in place by polypropylene plugs glued on the plate covers, while copper plates (1 cm x 1 cm) were sealed on the bottom of the wells. The silicone sealant was applied as a circular drop 12 mm in diameter. To each well, 3 ml of the chondrocyte suspension was added to yield the concentration of $10^5$ cells $cm^{-2}$. After 48 and 96 h of incubation in a humidified 5 % $CO_2$ incubator at 37$^{o}$C, the investigated samples and the medium were removed and inhibition zones were analyzed by using an optical microscope (Olympus CX41RF, Tokyo, Japan). Concentrations of $Ag^+$ and $Cu^{2+}$ released in the medium as well as concentrations of silver remained in the nanocomposite discs were determined by atomic absorption spectroscopy (AAS).

Bioreactor tissue cultures

Three bioreactor cartridges were loaded each with a *HG* Ag/alginate disc over an articular cartilage explant and dynamic compression was performed for 4 days. It should be noted that the applied displacement of 0.2 mm corresponded to approximately 10 % strain of the Ag/alginate disc. The experiment was repeated two times.

**Silver release from Ag/alginate discs under bioreactor and static conditions**

In order to examine differences in the release kinetics of AgNPs and/or ions from *HG* Ag/alginate discs in cytotoxicity studies under applied dynamic compression and in static monolayer cell cultures, a parallel study was performed under the same conditions. Three bioreactor cartridges were loaded each with a *HG* Ag/alginate disc placed over a PVA/PVP disc imitating the articular cartilage explant. The recirculation loops were filled each with 14 ml of the culture medium. The experiment lasted for 7 days with a daily medium replacement. A static study was performed in 6 well plates using three Ag/alginate discs in 14 ml of the culture medium, each, and daily medium replacements. All medium samples were analyzed for silver concentration.

**Analytical methods**

UV–Vis spectroscopy

Presence of AgNPs in Ag/alginate solutions as well in Ag/alginate discs upon dissolution was confirmed by UV-Vis spectroscopy using a 3100 spectrophotometer (Mapada, China). Ag/alginate solutions were diluted with water, while Ag/alginate discs were dissolved in 10 % w/v sodium citrate solution, using the ratio 0.1 g of the nanocomposite in 2.9 ml, in both cases.

Transmission electron microscopy (TEM)

Size and shape of AgNPs were analyzed by TEM using a JEM-1400 transmission electron microscope (JEOL Ltd. Tokyo, Japan). AgNP size distributions were determined based on measurements of 100 – 300 nanoparticles taken from different spots on the grid.

Fourier transform infrared spectroscopy (FTIR)

Samples of *HG* and *LG* Na-alginate solutions, and corresponding Ca-alginate hydrogels, Ag/alginate colloid solutions and Ag/alginate discs were dried and prepared in the form of KBr

pellets. The IR spectra were recorded in the transmission mode between 400 and 4000 $cm^{-1}$ using a Bomem MB-102 FTIR spectrometer (Quebec, Canada) with a resolution of 4 $cm^{-1}$.

Silver and copper concentrations

Silver concentrations in Ag/alginate discs and culture medium, as well as concentrations of released Cu(II) ions during the contact test were determined at four-digit accuracy by atomic absorption spectroscopy (AAS) using a Perkin Elmer 3100 spectrometer (Perkin Elmer, MA,USA), as described in the Supplementary material.

Histology

The upper edge of articular cartilage explants exposed to Ag/alginate discs in direct contact in the bioreactor culture was marked to observe possible effects of the tissue exposure to the nanocomposite. Preparation of the histological samples was performed by a standard procedure[37] described in the Supplementary material.

## RESULTS

### Production of Ag/alginate colloid solutions and discs

In this work, AgNPs were electrochemically produced in low viscosity and in medium viscosity Na-alginate solutions with different contents of G units (*HG* and *LG* colloid solutions, respectively). Both colloid solutions were then used to produce Ag/alginate discs and the presence of AgNPs in all samples was confirmed by UV-Vis spectroscopy and TEM analyses (Figs. 1 and 2, respectively).

All samples exhibited absorption maxima at wavelengths in the range 405 - 413 nm corresponding to silver nanoparticles.[38,39] Higher and narrower peaks obtained for the *HG*

alginate (Fig. 1a) indicate higher AgNP concentration at the narrower distribution as compared to the *LG* alginate (Fig. 1b). Dilution of colloid solutions induced approximately proportional decreases in the absorbance maxima values in both alginates. However, Ag/alginate discs exhibited higher absorption maxima than the corresponding starting colloids indicating higher AgNP concentrations (Fig. 1). This finding can be explained by alginate gel contraction during 48 h of gelling as reported previously.[26,40,41] It should be noted that the absorbance maximum increase and corresponding gel contraction were significantly higher in the case of *HG* alginate as compared to the *LG* alginate (~2.5- *vs*. ~1.4-fold increase, respectively, Fig. 1). Significant gel contraction and water expelling in *HG* alginate can be attributed to the higher G/M ratio, responsible for better crosslinking within the polymer hydrogel.[24,42] Results obtained by UV-Vis spectroscopy were confirmed by measurements of total silver concentrations by AAS amounting to 2.28 ± 0.12 mM and 1.29 ± 0.19 mM for *HG* and *LG* Ag/alginate discs, respectively.

TEM analysis confirmed the presence of spherical AgNPs in both colloid solutions (Fig. 2a,c). In addition, AgNPs were preserved and unchanged in Ag/alginate discs after gelling (Fig. 2b,d). The nanoparticle size distribution analysis complemented the UV-Vis spectroscopy findings, confirming smaller AgNPs at a narrower distribution in the *HG* colloid solution (Fig. 3a) as compared to those in the *LG* colloid (Fig. 3b). In the first case, AgNPs were in the range 3-18 nm with the average diameter of 8.7 ± 2.6 nm, which were retained in dissolved corresponding *HG* Ag/alginate discs (the size range was 4-14 nm with the average diameter of 8.2 ± 2.1 nm). These results indicate high stabilization of AgNPs in the *HG* colloid solution without visible agglomeration during alginate gelling. Conversely, a broader AgNP distribution in the range 3-

28 nm was found in the *LG* colloid with the average diameter of 9.3 ± 3.2 nm. The size distribution for dissolved *LG* Ag/alginate discs was in the same range (4 to 28 nm) (Fig. 3b) with the average diameter of 11.9 ± 4.8 nm implying slight agglomeration during gelling of this colloid solution.

Differences between alginates, Ca-alginate hydrogels, colloid solutions and corresponding Ag/alginate discs on the molecular level were examined by FTIR spectroscopy (Table 1). Comparison of IR spectra of hydrogels and alginates revealed major shifts in characteristic absorption bands for the –OH stretching vibration, and symmetric and asymmetric $COO^-$ stretching vibrations. In specific, the characteristic absorption band corresponding to –OH stretching vibration at ~3440 $cm^{-1}$ shifted to lower wavenumbers (~3426, ~3430, ~3426 and ~3413 $cm^{-1}$ for *LG* Ca-alginate, *HG* Ca-alginate, *LG* Ag/alginate discs and *HG* Ag/alginate discs, respectively), which indicates stronger interactions between hydroxyl groups in all hydrogels, especially in *HG* Ag/alginate discs. This result could be associated with the increase in polymer concentration after gelling as suggested in literature.[43] Shift of this characteristic band to a lower wavenumber (~3431 $cm^{-1}$) was also noticed in the *LG* colloid solution probably due to interactions of hydroxyl groups with AgNPs[44], while in the *HG* colloid solution this band remained unchanged. The exchange of $Na^+$ with $Ca^{2+}$ in all hydrogel forms resulted in a stronger C=O bond and consequently higher bond energy, leading to a small shift in stretching vibrations of carboxylate groups to higher wavenumbers.[45] Significant changes in asymmetric $COO^-$ stretching vibrations were observed in the *HG* colloid solution and *HG* Ag/alginate discs, which could be attributed to the presence of AgNPs. Overall, the obtained spectra could indicate possible differences in AgNP stabilization by different alginate compositions.

**Stability of Ag/alginate discs under bioreactor conditions**

Stability and mechanical properties of Ag/alginate discs (*LG* and *HG*) were evaluated in the biomimetic bioreactor under physiological dynamic compression and perfusion of the cell culture medium for up to 7 days. Up to the applied strain, the discs exhibited linear behavior as expected for alginate hydrogels[46], allowing determination of the dynamic compression moduli from the slopes of best linear fits of the stress - strain curves (Fig. 4). Significant differences between the investigated Ag/alginate discs were noticed so that, the *LG* discs exhibited inferior initial mechanical properties with the dynamic compression modulus of 43.7 ± 1.5 kPa as compared to *HG* discs, which exhibited the compression modulus of 64.3 ± 3.3 kPa (Fig. 4). This result is in accordance with the findings of significant *HG* hydrogel contraction during gelling and a significant increase in silver concentration indicating the increase in the polymer concentration as well. After 12 h period, mechanical properties decreased by approximately 34 % yielding dynamic compression moduli of 28.3 ± 0.6 kPa and 42.8 ± 1.5 kPa for *LG* and *HG* Ag/alginate discs, respectively, as a consequence of the gel network weakening due to the exchange of $Ca^{2+}$ with $Na^{+}$ from the culture medium. After 24 h the mechanical properties further decreased by ~74 % for *LG* and ~66 % for *HG* discs yielding dynamic compression moduli of 11.3 ± 1.0 kPa and 21.5 ± 2.1 kPa, respectively. Additionally, the stress-strain curve for *LG* discs significantly deviated from the linear trend ($r^2$<0.5). Consequently, after 36 h *LG* Ag/alginate discs lost the integrity, while the *HG* Ag/alginate discs retained the approximately constant compression modulus until the end of the experiment at day 7 (24.5 ± 0.7 kPa). Thus, the physiologically relevant bioreactor characterization unquestionably defined *HG* Ag/alginate discs as potential candidates for articular cartilage implants discarding the *LG* hydrogel as a

quickly degradable in the physiological environment. However, the *LG* hydrogel may be suitable as a wound dressing providing quick absorption of the exudates and releasing the AgNPs in 2 days, a period suitable for the wound dressing exchange. Thus, the *HG* Ag/alginate hydrogels were further evaluated with respect to cytotoxicity and silver release kinetics under dynamic compression relevant for articular cartilage.

**Cytotoxicity studies in monolayer cell cultures**

Cytotoxicity of *HG* Ag/alginate discs (initial total silver concentration of 2.28 ± 0.12 mM) in a direct test revealed moderate cytotoxic effects in monolayers of bovine calf chondrocytes. The silicone sealant was shown to be a suitable biocompatible material since the cells adhered uniformly around the material and covered the whole available surface, maintaining the characteristic fibroblast-like morphology typical for chondrocytes in monolayers[47] (Fig. 5a; Supplementary material, Fig. S2a). This result was basically identical as the appearance of the control monolayer culture (Supplementary material, Fig. S1). On the other hand, copper plates were shown to be cytotoxic after 48 h, inducing an inhibition zone of about 4 - 6 mm surrounded by a zone of rather rounded and contracted cells followed by a narrow zone next to the well edges of viable cells displaying normal morphology (Supplementary material, Fig. S2b). Furthermore, cytotoxicity of copper plates was even more evident after 96 h yielding an inhibition zone of 10 – 12 mm and a very small number of viable cells next to the well edges (Fig. 5b). In comparison, Ag/alginate discs induced less pronounced cytotoxic effects so that viable cells could not be detected next to the discs while a layer of viable cells next to the well

edges was wider (Supplementary material, Fig. S2c). The inhibition zone in this case was 1 – 2 mm and stayed approximately the same after 96 h (Fig. 5c).

The obtained data for Ag/alginate discs can be related to released silver concentrations in the culture medium, which were measured by AAS as 0.010 ± 0.001 mM and 0.016 ± 0.001 mM after 48 and 96 h, respectively. In the same time, released $Cu^{2+}$ concentrations in the cultures with copper plates were measured by AAS as 5.11 ± 0.61 mM and 4.95 ± 0.78 mM after 48 and 96 h, respectively. These results imply that although the released silver concentration slightly increased over time, it did not induce additional effects on cell survival contrary to the cultures with copper plates, in which the cell survival decreased. The observed findings may be attributed to formation of AgCl in the culture medium, as suggested previously[48,49], which is significantly less toxic than either AgNPs or $Ag^{+}$.[50]

**Cytotoxicity studies in 3D tissue cultures**

Cytotoxicity studies of *HG* Ag/alginate discs in the bioreactor over 4 days of compression demonstrated preserved cartilage explants identical as control static explant cultures. Histological examination of tissue cross-sections revealed uniformly distributed live cells and GAG in both cultures (Fig. 6b,c). In addition, a special attention was made to mark the upper and the lower sides of explants in the bioreactor in order to reveal potential effects of the direct contact with the Ag/alginate hydrogel. Again, histological analysis has shown that both explant sides were the same and appearances of all samples matched those of the initial native cartilage tissue (Fig. 6a). It should be noted that the dynamic compression in the bioreactor was exhibited on Ag/alginate discs while the strains occurring in explants were probably lower.

Medium flowrate of 0.12 ml/min corresponds to the superficial velocity of 18 µm/s calculated with respect to the disc base area, which is in the range of blood velocities in capillaries of 10 – 100 µm/s. Although the adult articular cartilage is largely avascular some fluid flow arises during cartilage compression in the course of daily activities[51,52], while in tissue engineering applications medium flow is required for efficient mass transport to the cells (e.g. [53,54]). The applied velocity of 18 µm/s would not induce negative effects on cell viability according to previous findings that the velocity of the smallest turbulent eddies of 0.4 cm/s was not damaging chondrocytes[55]. Furthermore, the explants were protected from the medium flow by the Ag/alginate discs so that it could be assumed that the bioreactor environment was adjusted to support the tissue culture and to reveal only the effects of the investigated material.

**Silver release from Ag/alginate discs under bioreactor and static conditions**

Silver release kinetics significantly differed under static and dynamic compression conditions (Fig. 8) so that the final released silver concentrations in the medium were 6.75 ± 0.56 and 4.86 ± 0.47 µM, respectively. These concentrations correspond to 12.3 % and 9.4 % of the initial AgNP content in Ag/alginate discs, respectively. Also the penetrated silver content into PVA/PVP discs was determined by AAS as 0.033 ± 0.020 mM, corresponding to 2.7 ± 0.9 nmol of AgNPs/$Ag^+$ per the disc (0.4 % of the total initial silver content in the Ag/alginate discs). Accordingly, Ag/alginate discs under bioreactor conditions retained higher AgNP content (515 ± 105 nmol) as compared to those in the static culture (343 ± 32 nmol). Higher silver release under static conditions occurred due to free swelling of the discs allowing easier ion exchange and weakening of the polymer network. Over 7 days under static conditions, disc weight and

volume increased ~3- and 4-fold, respectively (initial discs: 310 ± 20 mg, 12 mm in diameter, 2 mm thick; after 7 days: 950 ± 30 mg, ~17 mm in diameter, 4 mm thick). On the other hand, discs in the bioreactor study were constricted in the cartridges between the diaphragm and the PVA/PVP disc beneath, so that the disc size was practically retained with a moderate increase in weight (from 300 ± 10 mg to 500 ± 70 mg).

In order to reveal differences in the silver release, simple kinetics modeling was applied in both cases with the account of different phenomena in the two systems schematically represented in Figure 7. In specific, in the static culture silver release was governed by diffusion only, so that the one dimensional internal diffusion model can be applied[56]:

$$\frac{\partial c_n}{\partial t} = D'\left(\frac{\partial^2 c_n}{\partial x^2}\right) \quad (1)$$

where $x$ is the axial coordinate, $c_n$ is the silver concentration within the Ag/alginate discs and $D'$ is the apparent diffusion coefficient of AgNPs/$Ag^+$ in the swelled alginate matrix.

Since the disc swelling was relatively fast (within 24 h), a constant disc dimensions of 17 mm in diameter and 4 mm thickness were assumed. The released silver concentration in medium over time, $c_m$ is calculated as a difference between the initial silver content in the discs $c_o$ and the average silver content in discs at each time point, $\langle c_n \rangle$ [61]:

$$c_m = \frac{(c_o - \langle c_n \rangle)V}{V_m} \quad (2)$$

where $V$ is the disc volume and $V_m$ is the medium volume in the system. The average silver concentration within the disc at each time point can be calculated by the equation[61]:

$$\langle c_n \rangle = \frac{1}{X}\int_0^X c_n(x)dx \quad (3)$$

where *X* is the disc thickness.

Initially, AgNPs are uniformly distributed throughout the discs at the initial concentration $c_{0,}$ while AgNPs are not present in the medium. Silver concentration in the medium was assumed to be negligible throughout the experiment so that the inlet boundary condition at the upper disc surface at *x=0* was set as $c_n$=0 while the Neumann boundary condition (zero flux) was assumed at the outlet boundary since the disc was placed on the dish bottom:

$$\frac{\partial c_n}{\partial x} = 0 \text{ for } x = X \quad (4)$$

The equations (2-4) were solved numerically using MatLab, based on the backward finite difference method. The apparent diffusion coefficient, *D*' was determined by the least squares fit of the experimental data. Figure 8 shows satisfactory agreements between model predictions and the experimental data (RSD = 18 %). The apparent diffusion coefficient of AgNPs/$Ag^+$ within the swelled alginate matrix under static conditions was calculated as 5.3 x $10^{-13}$ $m^2/s$.

In the bioreactor, the discs were dynamically compressed, which induced repeated deformation and relaxation and, consequently, fluid flow in and out of the discs as schematically represented in Figure 7b. Thus, a convective transport of AgNPs and/or ions by a net flow can be assumed in addition to diffusion as it was also reported in literature for solute transport in hydrogels and cartilage tissue under dynamic compression.[57-60] In the present case,

compression induced the fluid inflow from the upper surface while during the disc relaxation the fluid left through the same surface so that one dimensional transport was assumed again. It should be noted that probably some fluid was leaving also through the lateral surface but for the simplicity reasons one dimensional model was adopted here. The change in AgNP concentration within the Ag/alginate discs, $c_n$ was described by the Eq. (1) with addition of the advection term yielding the advection-diffusion equation as also used previously[61]:

$$\frac{\partial c_n}{\partial t} = D''\left(\frac{\partial^2 c_n}{\partial x^2}\right) - u\frac{\partial c_n}{\partial x} \quad (5)$$

where $x$ is the axial coordinate, $u$ is the net fluid velocity through the disc and $D''$ is the apparent diffusion coefficient of AgNPs/$Ag^+$ in Ag/alginate discs that negligibly swelled.

Again, Eq. (5) was simultaneously solved with equations (2-4) using MatLab, while the apparent diffusion coefficient and the net fluid velocity through the discs were model parameters determined by the least squares fit of the experimental data. The net flux through the bottom disc boundary was again set to 0 (Eq. (4)) based on negligible silver amount that diffused into PVA/PVP discs (<5 % of the total amount of released silver). The model predictions were in satisfactory agreements with the experimental data (RSD = 17%, Fig. 8) yielding the apparent diffusion coefficient of 1.4 x $10^{-17}$ $m^2/s$ and the net fluid velocity of 3.9 x $10^{-10}$ m/s.

**DISCUSSION**

The aim of this work was to use a biomimetic bioreactor for functional characterization of Ag/alginate nanocomposite hydrogels under physiologically relevant conditions in order to evaluate potentials regarding the particular application as articular cartilage implants. In

specific, two alginate types were used with different ratios of G and M units. AgNPs were successfully synthesized in solutions of both alginate types with slightly smaller AgNPs at a narrower distribution in the alginate with a higher content of G units (*HG* alginate). This result can be probably explained by a more favorable spatial conformation of G units and GG blocks. In specific, it was shown that AgNPs stabilized by electrostatic interactions with a capping agent, such as alginate, have negative ζ potentials.[62] Interactions of cations with carboxyl groups have been shown to decrease the ζ potential and increase the tendency for agglomeration of NPs, which has led to the assumption that carboxyl groups may have a critical role in NP stabilization.[63] Results of FTIR analyses in the present study are in accordance with this hypothesis showing changes in asymmetric $COO^-$ stretching vibrations in the *HG* colloid solution due to the presence of AgNPs. Some studies suggested that AgNPs could be also stabilized by electrostatic interactions with negatively charged ring oxygen, as well as by interactions with free hydroxyl groups.[15,64] Therefore, it could be supposed that the suitable conformation of functional groups in G units as well as in polyguluronate blocks are probably responsible for better stabilization of synthesized AgNPs than by polymannuronate blocks, similarly as it was shown for $Ca^{2+}$ binding.[65] However, both colloid solutions yielded Ag/alginate hydrogels with preserved AgNPs. Still, the AgNP size was preserved during gelation in *HG* Ag/alginate in contrast to the *LG* Ag/alginate in which it slightly increased (for ~25 %). This result indicates again better stabilization of AgNPs within alginates with higher contents of G units. In parallel, *HG* hydrogels shrunk significantly more during gelation than *LG* hydrogels due to stronger bonds of $Ca^{2+}$ to GG blocks forming a well-known "egg-box" model.[65] As a consequence, the alginate concentration increased, yielding also mechanically stronger

hydrogels. This result is expected as it was reported in literature that alginates rich in G units form stronger and more stable gels than alginates rich in M units.[36,66,67] However, to distinguish potentials of the obtained Ag/alginate discs (*HG* and *LG*) for implantation in soft tissues, such as articular cartilage, functional characterization was performed regarding mechanical stability, cytotoxicity and release kinetics under relevant conditions in a biomimetic bioreactor. In specific, 10 % strain was selected based on physiological deformation of cartilage under loading, estimated to be ~20 % or less.[29] The applied loading frequency of 0.84 Hz is close to 1 Hz, which correlates to the walking cycle[68] and was reported to generally stimulates chondrogenesis.[69] Dynamic compression modulus determined in the biomimetic bioreactor for the *HG* nanocomposite hydrogel (~64 kPa) was almost 50 % higher than that determined for the *LG* nanocomposite hydrogel (~44 kPa). The obtained values are in agreement with the values reported in literature (Table 2). Generally at higher compression rates, higher compression moduli are obtained, as expected, while it is clear that mechanical properties of alginate hydrogels are strongly influenced by alginate composition as well as the concentration and nature of the gelling cation, gelation period, etc.[73-75] Also, in the presence of $Na^+$, weakening of Ca-alginate hydrogels is expected due to ion exchange. Consequently, the compression modulus of the *LG* nanocomposite steadily decreased in the culture medium over time until 36 h, when the discs lost their integrity. On the contrary, the compression modulus of *HG* discs decreased over the first 24 h to ~24 kPa, after which period the modulus value stayed constant until the end of experiment at day 7. Thus, the biomimetic bioreactor characterization clearly quantified differences between the two hydrogel types pointing towards suitable applications. Namely, Ag/alginate discs derived from the alginate rich in G units are designated as potential

candidates for articular cartilage implants while alginates rich in M units are potentially suitable for wound treatments rapidly dissolving and releasing AgNPs.

Cytotoxicity studies of *HG* Ag/alginate discs in standard 2D chondrocyte monolayers and in 3D bioreactor cartilage tissue cultures revealed contrary results. While moderate cytotoxic effects were detected in the direct contact with cells in monolayers, at the same time, unchanged histological appearances of cartilage explants in direct contact with the discs were observed after 4 days of dynamic compression. These results are in accordance with literature findings that cells in 2D cultures are more sensitive to NPs as compared to cells in a 3D environment, which are protected by the ECM.[76] The ECM provides cell-tissue interactions, normal cell morphology and also a physical barrier for penetration of nanoparticles.[77] It should be added that similar Ag/alginate hydrogels in the form of microfibers were shown to promote wound healing in a rat burn model without adverse effects.[78,79] Thus, the biomimetic bioreactor environment provided results closer to the *in vivo* findings than the 2D culture. Furthermore, as compared to spheroid cell cultures, often used as 3D models (e.g.[80,81]), explant cultures applied in the present study provided the native tissue structure and composition closely resembling the *in vivo* situation.

Finally, the bioreactor characterization revealed also different mechanisms of AgNP release and disc behavior under biomimetic mechanical strains and under static, free swelling conditions. The apparent diffusion coefficient of AgNPs/$Ag^+$ obtained under static conditions ($5.3 \times 10^{-13}$ $m^2/s$) is in agreement with previously reported AgNP diffusion coefficients in biological tissues. In specific, the value of $3 \times 10^{-13}$ $m^2/s$ was assessed by single particle tracking and the Brownian

diffusion model in zebrafish embryos incubated with AgNPs (5–46 nm) under static conditions[82] while the values of $(4.3 – 4.6) \times 10^{-13}$ $m^2/s$ were obtained from permeability data for spherical AgNPs (50 nm) in the murine skin using the Franz diffusion cell[83]. The value determined in the present study was somewhat higher than the $Ag^+$ diffusion coefficient of $1.5 \times 10^{-14}$ $m^2/s$ determined in a Ag/PVA hydrogel immersed in a phosphate buffer pH=7, by the integral form of the Fick's diffusion model approximated for short times[84]. On the contrary, significantly lower diffusion coefficients of $AgNP/Ag^+$ of $4.6 \times 10^{-19}$ and $6.9 \times 10^{-19}$ $m^2/s$ were obtained in Ag/alginate microbeads in water under static conditions by applying the same diffusion model in differential form as in the present work[49,61]. Slower diffusion rates in these cases were expected due to higher stability of the polymer network in water as compared to the culture medium containing $Na^+$, which provokes the network swelling and, thus, diffusion enhancement.

Disc swelling was restricted in the bioreactor, while dynamic compression induced silver release by both diffusion and forced convection. These two effects induced decreased silver release as compared to free-swelling static conditions resulting in the apparent diffusion coefficient of $1.4 \times 10^{-17}$ $m^2/s$. According to the Reinhart - Peppas theory, diffusion coefficient values are directly proportional to the hydrogel swelling degree.[85] Additionally, matrix deformation due to dynamic compression could affect diffusion by reducing the hydrogel pores size and increasing the steric resistance[86] Previous experimental and mathematical modeling studies of silver release from Ag/alginate microbeads have implied that rapid hydrogel rehydration induced fast AgCl precipitation within the microbeads resulting in the lowest silver release.[49] Similarly, in the present study, the medium flow during the compression/decompression cycle could enhance

precipitation of AgCl within the discs. Still, the net fluid velocity was estimated to be very low of the order of magnitude of $10^{-10}$ m/s. Although this simplified model assumed one directional fluid flow neglecting the flow through the disc lateral surface the obtained velocity value is comparable to the interstitial fluid velocity of 3.14 x $10^{-10}$ m/s reported for a damaged articular cartilage tissue under a rolling load.[87] This result indicates again relevance of the bioreactor conditions applied.

**CONCLUSION**

Biomimetic bioreactors present adequate *in vitro* models for biomaterial evaluation regarding nanotoxicity in 3D tissue cultures along with providing possibilities for additional functional characterization such as mechanical stability or release kinetics under physiologically relevant conditions over prolonged periods of time. This approach facilitates profound understanding of the biomaterial behavior in an *in vivo*-like environment thus minimizing the number of necessary studies in animals. In the present work, a biomimetic bioreactor with dynamic compression was used as a tool for: i) assessment of different alginate types regarding potential applications, *ii*) evaluation of cytotoxicity of Ag/alginate nanocomposites in 3D cultures and *iii*) assessment of different mechanisms of nanoparticle release and hydrogel behavior under biomimetic conditions in comparison to static free-swelling conditions. The obtained results strongly confirmed the utility of such an approach clearly differentiating between two alginate types, which is especially relevant for exploitation of biomaterials from natural origins. Also, cytotoxicity studies proved higher sensitivity of cells in 2D cultures as compared to 3D bioreactor cultures, which were in accordance with results obtained previously *in vivo*. Thus, it

could be generally presumed that biomimetic bioreactors applying conditions suited to the environment of a particular organ or a tissue may provide realistic and reliable evaluation of functionality of biomaterials and especially nanomaterials.

**ACKNOWLEDGEMENTS**

This work was supported by the Ministry of Education, Science and Technological Development of the Republic of Serbia (Grant III 45019). The authors would like to thank Predrag Petrovic for FTIR analysis.

**CONFLICT OF INTEREST STATEMENT**

The authors have no conflicts of interest to declare in preparation of this manuscript.

**REFERENCES**

REFERENCES

1. Pourchez J, Forest V, Boumahdi N, Boudard D, Tomatis M, Fubini B, Herlin-Boime N, Leconte Y, Guilhot B, Cottier M, Grosseau P. In vitro cellular responses to silicon carbide nanoparticles: impact of physico-chemical features on pro-inflammatory and pro-oxidative effects. J Nanopart Res 2012;14:1143.

2. Cunningham S, Brennan-Fournet M, Ledwith D, Byrnes L, Joshi L. Effect of Nanoparticle Stabilization and Physicochemical Properties on Exposure Outcome: Acute Toxicity of Silver Nanoparticle Preparations in Zebrafish (Daniorerio). Environ Sci Technol 2013;47:3883-3892.

3. Dworak N, Wnuk M, Zebrowski J, Bartosz G, Lewinska A. Genotoxic and mutagenic activity of diamond nanoparticles in human peripheral lymphocytes in vitro. Carbon 2014;68:763-776.

4. Basu B. Biomaterial Science and Tissue Engineering: Principles and Methods. New York: Cambridge University Press; 2017.

5. Baek H, Yoo J, Rah D, Han D, Lee D, Kwon O, Park J. Evaluation of the Extraction Method for the Cytotoxicity Testing of Latex Gloves. Yonsei Med J 2005;46:579-583.

6. Joris F, Manshian B, Peynshaert K, De Smedt S, Braeckmans K, Soenen S. Assessing nanoparticle toxicity in cell-based assays: influence of cell culture parameters and optimized models for bridging the in vitro–in vivo gap. Chem Soc Rev 2013;42:8339-8359.

7. Comfort K, Braydich-Stolle L, Maurer E, Hussain S. Less Is More: Long-Term in Vitro Exposure to Low Levels of Silver Nanoparticles Provides New Insights for Nanomaterial Evaluation. ACS Nano 2014;8:3260-3271.

8. Luo Y, Wang C, Hossain M, Qiao Y, Ma L, An J, Su M. Three-Dimensional Microtissue Assay for High-Throughput Cytotoxicity of Nanoparticles. Anal Chem 2012;84:6731-6738.

9. Marquis B, Love S, Braun K, Haynes C. Analytical methods to assess nanoparticle toxicity. Analyst 2009;134:425-439.

10. Pampaloni F, Reynaud E, Stelzer E. The third dimension bridges the gap between cell culture and live tissue. Nat Rev Mol Cell Biol 2007;8:839-845.

11. Elliott, N. Yuan, F. A Review of Three-Dimensional In Vitro Tissue Models for Drug Discovery and Transport Studies. J Pharm Sci 2011;100:59-74.

12. Lee J, Han Y. Lee S. Long-Duration Three-Dimensional Spheroid Culture Promotes Angiogenic Activities of Adipose-Derived Mesenchymal Stem Cells. Biomol Ther 2016;24:260-267.

13. Engelmayr G, Hildebrand D, Sutherland F, Mayer J, Sacks M. A novel bioreactor for the dynamic flexural stimulation of tissue engineered heart valve biomaterials. Biomaterials 2003;24:2523-2532.

14. Stojkovska J, Bugarski B, Obradovic B. Evaluation of alginate hydrogels under in vivo–like bioreactor conditions for cartilage tissue engineering. J Mater Sci: Mater Med 2010;21:2869-2879.

15. Jovanovic Z, Stojkovska J, Obradovic B, Miskovic- Stankovic V. Alginate hydrogel microbeads incorporated with Ag nanoparticles obtained by electrochemical method. Mat Chem Phys 2012;133:182–189.

16. Obradovic B, Miskovic-Stankovic V, Jovanovic Z, Stojkovska J. Production of alginate microbeads with incorporated silver nanoparticles. patent RS53508 (B1), 2015.

17. Haug A, Larsen B, Smidsrod O. Uronic acid sequence in alginate from different sources. Carbohydr Res 1974;32:217-225.

18. Jørgensen T, Sletmoen M, Draget K. Stokke B. Influence of Oligoguluronates on Alginate Gelation, Kinetics, and Polymer Organization. Biomacromolecules 2007;8:2388-2397.

19. Sari-Chmayssem N, Taha S, Mawlawi H, Guégan J, Jeftić J, Benvegnu T. Extracted and depolymerized alginates from brown algae Sargassumvulgare of Lebanese origin: chemical, rheological, and antioxidant properties. J Appl Phycol 2015;28:1915-1929.

20. Lee K, Mooney D. Alginate: Properties and biomedical applications. Prog Polym Sci 2012;37:106-126.

21. Hay I, Rehman Z, Moradali M, Wang Y, Rehm B. Microbial alginate production, modification and its applications. Microb Biotechnol 2013;6:637–650.

22. Draget KI, Taylor C. Chemical, physical and biological properties of alginates and their biomedical implications. Food Hydrocoll 2011;25:251–256.

23. Donati I, Paoletti S. Material Properties of Alginates. In: Rehm B. editor. Alginates: biology and applications. Berlin Heidelberg: Springer, 2009.

24. Topuz F, Henke A, Richtering W, Groll J. Magnesium ions and alginate do form hydrogels: a rheological study. Soft Matter 2012;8:4877-4881.

25. Zvicer J, Samardzic M, Miskovic-Stankovic V, Obradovic B. Cytotoxicity studies of Ag/alginate nanocomposite hydrogels in 2D and 3D cultures. In Bioinformatics and Bioengineering (BIBE) 2015; IEEE 15th International Conference on 2015:1-6.

26. Stojkovska J, Zvicer J, Jovanovic Z, Miskovic-Stankovic V, Obradovic B. Controlled production of alginate nanocomposites with incorporated silver nanoparticles aimed for biomedical applications. J Serb Chem Soc 2012;77:1709-1722.

27. Freed LE, Marquis JC, Nohria A, Emmanual J, Mikos AG, Langer R. Neocartilage formation in vitro and in vivo using cells cultured on synthetic biodegradable polymers. J Biomed Mater Res 1993;27:11–23.

28. Petrovic M, Mitrakovic D, Bugarski B, Vonwil D, Martin I, Obradovic B. A novel bioreactor with mechanical stimulation for skeletal tissue engineering. Chem Ind Chem Eng Q 2009;15:41-44.

29. Mauck RL, Soltz MA, Wang CCB, Wong DD, Chao P-HG, Valhmu WB, Hung CT, Athesian GA. Functional tissue engineering of articular cartilage through dynamic loading of chondrocyte-seeded agarose gels. J Biomech Eng 2000;122:252–260.

30. Mauck RL, Byers BA, Yuan X, Tuan RS. Regulation of cartilaginous ECM gene transcription by chondrocytes and MSCS in three-dimensional culture in response to dynamic loading. Biomech Model Mechanobiol 2007;6:113–125.

31. Demarteau O, Wendt D, Braccini A, Jakob M, Schäfer D, Heberer M, Martin I. Dynamic compression of cartilage constructs engineered from expanded human articular chondrocytes. Biochem Biophys Res Commun 2003;310:580–588.

32. Hoenig E, Winkler T, Mielke G, Paetzold H, Schuettler D, Goepfert C, Machens H, Morlock M, Schilling A. High amplitude direct compressive strain enhances mechanical properties of scaffold-free tissue-engineered cartilage. Tissue Eng Part A 2011;17:1401–1411.

33. Jovanović Ž, Radosavljević A, Kačarević-Popović Z, Stojkovska J, Perić-Grujić A, Ristić M, Matić I, Juranić Z, Obradovic B, Mišković-Stanković V. Bioreactor validation and biocompatibility of Ag/poly(N-vinyl-2-pyrrolidone) hydrogel nanocomposites. Colloids Surf B: Biointerfaces 2013;105:230-235.

34. Obradovic B, Stojkovska J, Jovanovic Z, Miskovic-Stankovic V. Novel alginate based nanocomposite hydrogels with incorporated silver nanoparticles. J Mater Sci: Mater Med 2012;23:99-107.

35. Seucedo-Zeni N, Mewes S, Niestroj R, Gasiorowski L, Murawa D, Nowaczyk P, Tomasi T, Weber E, Dworacki G, Morgenthaler N, Jansen H, Propping C, Sterzynska K, Dysykiewich W, Zabel M, Kiechle M, Reuning U, Schmitt M, Lucke K. A novel method for the in vivo isolation of circulating tumor cells from peripheral blood of cancer patients using a functionalized and structured medical wire. Int J Oncol 2012;41:1241-1250.

36. Briganti E, Losi P, Raffi A, Scoccianti M, Munaò A, Soldani G. Silicone based polyurethane materials: a promising biocompatible elastomeric formulation for cardiovascular applications. J Mater Sci Mater Med 2006;17:259-266.

37. Park H, Choi B, Hu J, Lee M. Injectable chitosan hyaluronic acid hydrogels for cartilage tissue engineering. Acta Biomater 2013;9:4779-4786.

38. Mulfinger L, Solomon S, Bahadory M, Jeyarajasingam A, Rutkowsky S, Boritz, C. Synthesis and Study of Silver Nanoparticles. J Chem Edu 2007;84:322-325.

39. Martínez-Castañón G, Niño-Martínez N, Martínez-Gutierrez F, Martínez-Mendoza J, Ruiz F. Synthesis and antibacterial activity of silver nanoparticles with different sizes. J Nanopart Res 2008;10:1343-1348.

40. Martinsen, A, Skjåk-Braek, G. Smidsrød, O. Alginate as immobilization material: I. Correlation between chemical and physical properties of alginate gel beads. Biotechnol Bioeng 1989; 33:79-89.

41. Velings N, Mestdagh M. Physico-chemical properties of alginate gel beads. Pol Gels Netw 1995;3:311-330.

42. Davidovich-Pinhas M, Bianco-Peled H. A quantitative analysis of alginate swelling. Carbohydr Polym 2010;79:1020-1027.

43. Zechner-Krpan V, Petravić-Tominac V, Gospodarić I, Sajli L, Đaković S, Filipović-Grčić J. Characterization of â-glucans isolated from brewer's yeast and dried by different methods. Food Technol Biotechnol 2010;48:189-197.

44. Zhao X, Xia Y, Li Q, Ma X, Quan F, Geng C, Han Z. Microwave-assisted synthesis of silver nanoparticles using sodium alginate and their antibacterial activity. Colloids Sur A: Physicochem Eng Asp 2014;444:180-188.

45. Sartori C, Finch D, Ralph B, Gilding K. Determination of the cation content of alginate thin films by FTi.r. spectroscopy. Polymer 1997;38:43-51.

46. Junter GA, Vinet F. Compressive properties of yeast cell-loaded Ca-alginate hydrogel layers: comparison with alginate–CaCO3 microparticle composite gel structures. Chem Eng J 2009;145:514–21.

47. Glowacki J, Trepman E, Folkman J. Cell shape and phenotypic expression in chondrocytes, Proc Soc Exp Biol Med 1983;172:93–98.

48. Stojkovska J, Kostic D, Jovanovic Z, Vukasinovic-Sekulic M, Miskovic-Stankovic V, Obradovic B. A comprehensive approach to in vitro functional evaluation of Ag/alginate nanocomposite hydrogels. Carbohydr Polym 2014;111:305-314.

49. Kostic D, Vidovic S. Obradovic B. Silver release from nanocomposite Ag/alginate hydrogels in the presence of chloride ions: experimental results and mathematical modeling. J Nanopart Res 2016;18:76:1-16.

50. Angel B, Batley G, Jarolimek C, Rogers N. The impact of size on the fate and toxicity of nanoparticulate silver in aquatic systems. Chemosphere 2013;93:359-365.

51. Camarero-Espinosa S, Rothen-Rutishauser B, Foster E, Weder C. Articular cartilage: from formation to tissue engineering. Biomater Sci 2016;4:734-767.

52. Eckstein F, Tieschky M, Faber S, Englmeier K, Reiser M. Functional analysis of articular cartilage deformation, recovery, and fluid flow following dynamic exercise in vivo. Anat Embryol 1999;200:419-424.

53. Martin I, Wendt D, Heberer M. The role of bioreactors in tissue engineering. Trends Biotechnol 2004;22:80-86.

54. Forrestal, D., Klein, T. and Woodruff, M. (). Challenges in engineering large customized bone constructs. Biotechnol Bioeng 2017;114:1129-1139.

55. Vunjak-Novakovic G, Freed L, Biron R, Langer R. Effects of mixing on the composition and morphology of tissue-engineered cartilage. AIChE J 1996;42:850-860.

56. Lavoine N, Guillard V, Desloges I, Gontard N, Bras J. Active bio-based food-packaging: Diffusion and release of active substances through and from cellulose nanofiber coating toward food-packaging design. Carbohydr Polym 2016;149:40-50.

57. Chahine N, Albro M, Lima E, Wei V, Dubois C, Hung C, Ateshian G. Effect of Dynamic Loading on the Transport of Solutes into Agarose Hydrogels. Biophysic J 2009;97:968-975.

58. Evans R, Quinn T. Dynamic Compression Augments Interstitial Transport of a Glucose-Like Solute in Articular Cartilage. Biophys J 2006;91:1541-1547.

59. Albro M, Chahine N, Li R, Yeager K, Hung C, Ateshian G. Dynamic loading of deformable porous media can induce active solute transport. J Biomechan 2008;41:3152-3157.

60. Bonassar L, Grodzinsky A, Frank E, Davila S, Bhaktav N, Trippel S. The effect of dynamic compression on the response of articular cartilage to insulin-like growth factor-I. J Orthop Res 2001;19:11-17.

61. Kostic D, Malagurski I, Obradovic B. Transport of silver nanoparticles from nanocomposite Ag/alginate hydrogels under conditions mimicking tissue implantation. Hem Ind 2017;71:383-394.

62. Seo S, Lee G, Lee S, Jung S, Lim J, Choi J. Alginate-based composite sponge containing silver nanoparticles synthesized in situ. Carbohydr Polym 2012;90:109-115.

63. El Badawy A, Silva R, Morris B, Scheckel K, Suidan M, Tolaymat T. Surface Charge-Dependent Toxicity of Silver Nanoparticles. Environ Sci Technol 2011;45:283-287.

64. Montaser A, Abdel-Mohsen A, Ramadan M, Sleem A, Sahffie N, Jancar J, Hebeish A. Preparation and characterization of alginate/silver/nicotinamide nanocomposites for treating diabetic wounds. Int J Biol Macromol 2016;92:739-747.

65. Braccini I, Perez S. Molecular basis of Ca2+-induced gelation in alginates and pectins: The egg-box model revisited. Biomacromolecules 2001;2:1089-1096.

66. Draget K, Skjåk-Bræk G, Smidsrød O. Alginate based new materials. Int J Biol Macromol 1997;21:47-55.

67. Yang C, Wang M, Haider H, Yang J, Sun J, Chen Y, Zhou J, Suo Z. Strengthening Alginate/Polyacrylamide Hydrogels Using Various Multivalent Cations. ACS Appl Mater Interfeces 2013;5:10418-10422.

68. Stolk R, Wegen van der-Franken C Neumann H. A Method for Measuring the Dynamic Behavior of Medical Compression Hosiery during Walking. Dermatol Surg 2004;30:729-736.

69. Anderson DE, Johnstone B. Dynamic mechanical compression of chondrocytes for tissue engineering: A critical review. Front Bioeng Biotechnol 2017;5:no76:1-20.

70. Kuo C, Ma P. Ionically crosslinked alginate hydrogels as scaffolds for tissue engineering: Part 1. Structure, gelation rate and mechanical properties. Biomaterials 2001;22:511-521.

71. Aarstad O, Heggset E, Pedersen I, Bjørnøy S, Syverud K, Strand B. Mechanical Properties of Composite Hydrogels of Alginate and Cellulose Nanofibrils. Polymers 2017;9:378.

72. Draget K, Skjåk-Bræk G, Smidsrød O. Alginic acid gels: the effect of alginate chemical composition and molecular weight. Carbohydr Polym 1994;25:31-38.

73. Kaklamani G, Cheneler D, Grover L, Adams M, Bowen J. Mechanical properties of alginate hydrogels manufactured using external gelation. J Mech Behav Biomed Mater 2014;36:135-142.

74. Augst AD, Kong HJ, Mooney DJ. Alginate hydrogels as biomaterials. Macromol Biosci. 2006;6:623–633.

75. Growney Kalaf E, Pendyala M, Bledsoe J, Sell S. Characterization and restoration of degenerated IVD function with an injectable, in situ gelling alginate hydrogel: An in vitro and ex vivo study. J Mech Behav Biomed Mater 2017;72:229-240.

76. Lee J, Lilly G, Doty R, Podsiadlo P, Kotov N. In vitro Toxicity Testing of Nanoparticles in 3D Cell Culture. Small 2009;5:1213-1221.

77. Barua S, Mitragotri S. Challenges associated with penetration of nanoparticles across cell and tissue barriers: A review of current status and future prospects. Nano Today 2014;9:223-243.

78. Stojkovska J, Jovanović Ž, Jančić I, Bufan B, Milenković M, Mišković-Stanković V, Obradović B. Novel Ag/alginate nanocomposites for wound treatments: animal studies. Rane 2013;4:17–22.

79. Stojkovska J, Djurdjevic Z, Jancic I, Bufan B, Milenkovic M, Jankovic R, Miskovic-Stankovic V, Obradovic B. Comparative in vivo evaluation of novel formulations based on alginate and silver nanoparticles for wound treatments. J Biomater Appl 2018;32:1197-1211.

80. Gurumurthy B, Bierdeman P, Janorkar A. Spheroid model for functional osteogenic evaluation of human adipose derived stem cells. J Biomed Mater Res A 2017;105:1230-1236.

81. Kunz-Schughart L, Freyer J, Hofstaedter F. Ebner R. The Use of 3-D Cultures for High-Throughput Screening: The Multicellular Spheroid Model. J Biomol Screen 2004;9:273-285.

82. Lee K, Nallathamby P, Browning L, Osgood C, Xu X. In Vivo Imaging of Transport and Biocompatibility of Single Silver Nanoparticles in Early Development of Zebrafish Embryos. ACS Nano 2007;1:133-143.

83. Tak Y, Pal S, Naoghare P, Rangasamy S, Song J. Shape-Dependent Skin Penetration of Silver Nanoparticles: Does It Really Matter?. Sci Rep 2015;5:16908.

84. Krstić J, Spasojević J, Radosavljević A, Perić-Grujić A, Đurić M, Kačarević-Popović Z, Popović S. In vitro silver ion release kinetics from nanosilver/poly(vinyl alcohol) hydrogels synthesized by gamma irradiation. J Appl Polym Sci 2014;131:40321-40335.

85. Reinhart C, Peppas N. Solute diffusion in swollen membranes. Part II. Influence of crosslinking on diffusive properties. J Memb Sci 1984;18:227-239.

86. Greene G, Zappone B, Söderman O, Topgaard D, Rata G, Zeng H, Israelachvili J. Anisotropic dynamic changes in the pore network structure, fluid diffusion and fluid flow in articular cartilage under compression. Biomaterials 2010;31:3117-3128.

87. Sadeghi H, Shepherd D, Espino D. Effect of the variation of loading frequency on surface failure of bovine articular cartilage. Osteoarthr Cartil 2015;23:2252-2258.

**Figure captions**

Figure 1. UV-Vis absorption spectra of the initially synthesized 3.9 mM colloid solutions, heat-treated colloid solutions diluted to the nominal silver concentration of 1 mM and resulting Ag/alginate discs: a) low viscosity alginate with high G unit content (HG); b) medium viscosity alginate with low G unit content (LG); the spectra correspond to a 100 µl sample of either colloid solution in 2.9 ml of deionized water or 0.1 g of Ag/alginate discs in 2.9 ml of 10 w/v % sodium citrate; (data represent average of n=3)

Figure 2. TEM images: a) LG Ag/alginate colloid solution; b) LG Ag/alginate discs; c) HG Ag/alginate colloid solution; d) HG Ag/alginate discs.(scale bar: 100 nm)

Figure 3. Nanoparticle size distribution in: a) HG colloid solution and Ag/alginate discs, and b) LG colloid solution and Ag/alginate discs (measurements of at least 100 nanoparticles)

Figure 4. Experimentally determined and best linear fits of stress–strain relationships over time for LG Ag/alginate discs (a) and HG Ag/alginate discs (b) at a loading rate of 337.5 µm/s (data represent average of n = 3 smoothed by 5-point centered moving-average filter)

Figure 5. Monolayer chondrocyte cultures in the contact test after 96 h of exposure to: a) silicone sealant as a reference biocompatible material, b) copper plate as a reference toxic material, c) Ag/alginate disc. Left panels: material edges; right panels: edges of the wells (scale bar = 500 µm)

Figure 6. Histological cross-sections of cartilage tissue explants: a) initial native tissue, b) control static culture after 4 days, c) the bioreactor culture in contact with Ag/alginate discs after 4 days (left part presents the explant surface in direct contact with the disc, right part presents

the lower explant side). Left panels: alcian blue stain; right panels: H&E stain (scale bar = 500 μm)

Figure 7. Schematic presentation of silver release studies of Ag/alginate discs: experimental set up and geometry for mathematical modeling: a) static conditions – discs swelled from the initial thickness $X_0$= 2mm to the thickness $X$ = 4 mm; one dimensional diffusion of AgNPs/ions with the apparent diffusion coefficient $D'$; b) dynamic compression conditions – each disc was placed on top of a PVA/PVP disc allowing negligible swelling; one dimensional diffusion of AgNPs/ions with the apparent diffusion coefficient $D''$ accompanied with the convective fluid flow at the net velocity $u$ as a result of the fluid inflow during compression and outflow during relaxation

Figure 8. Silver concentration in the medium over 7 days under static and bioreactor dynamic compression conditions: experimental data (symbols) and modeling results (lines) (data represent average of n=3)

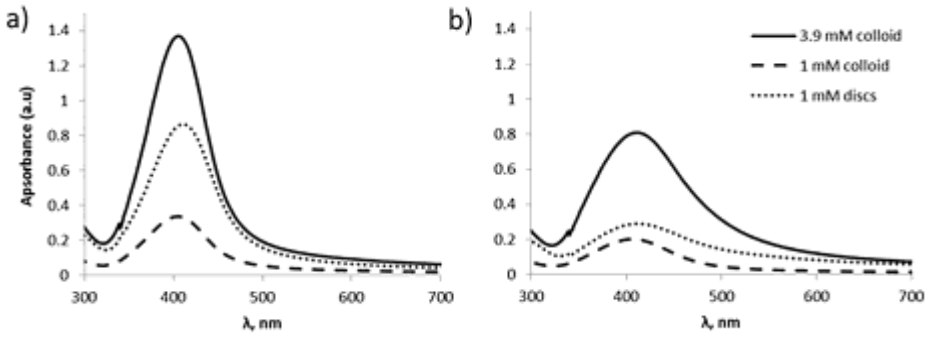

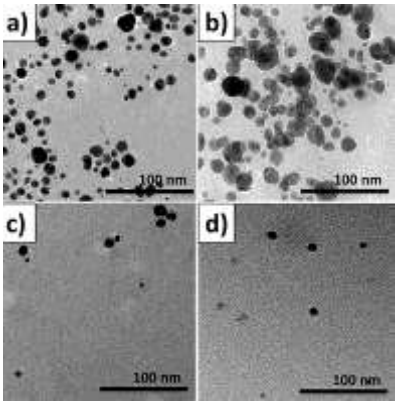


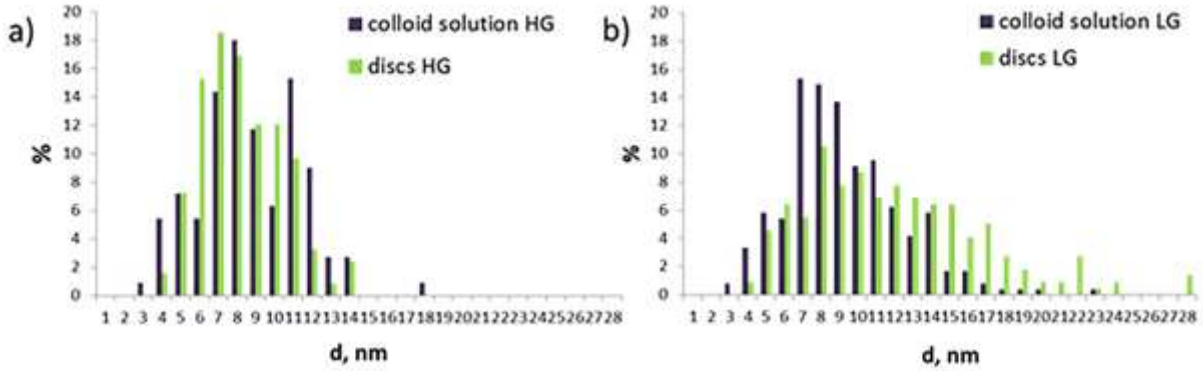


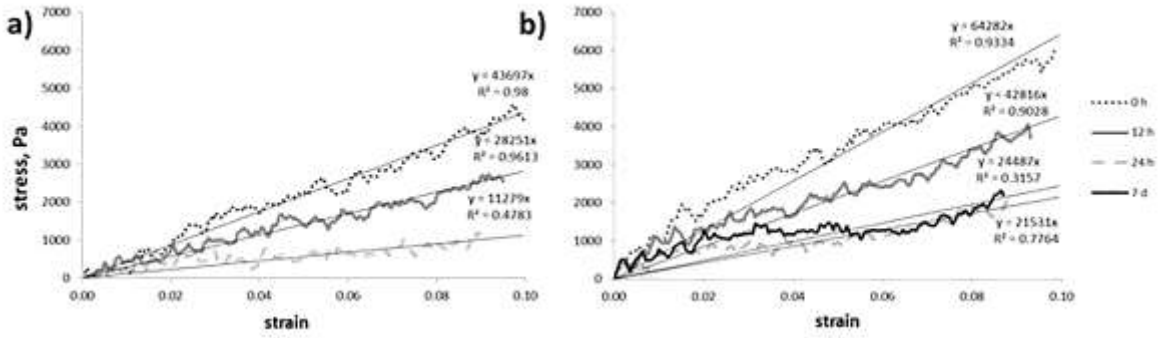


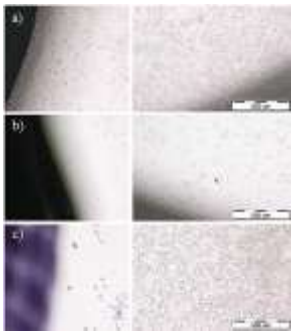

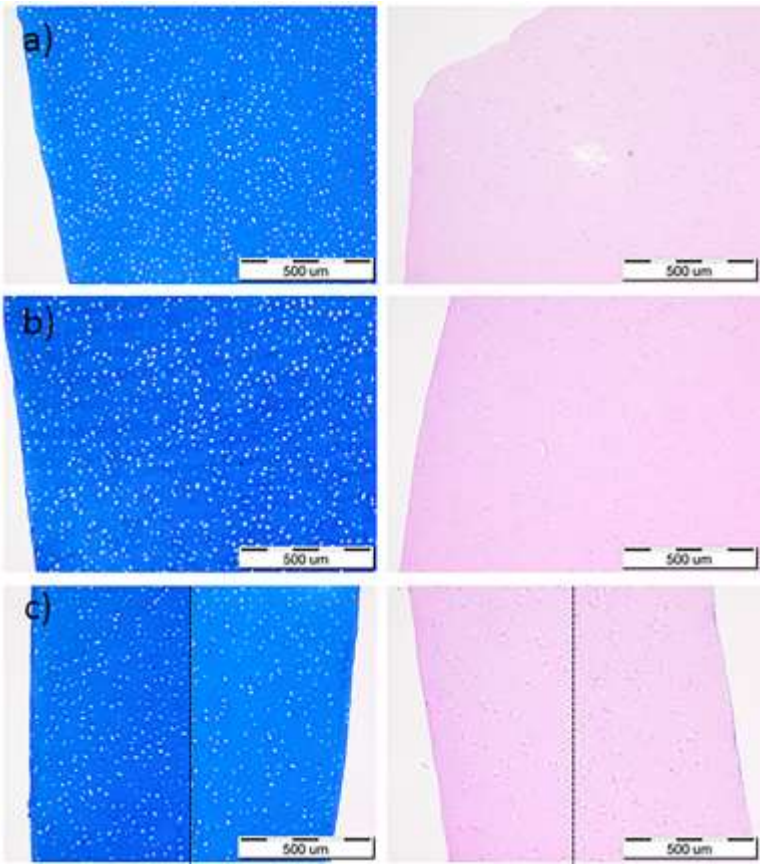


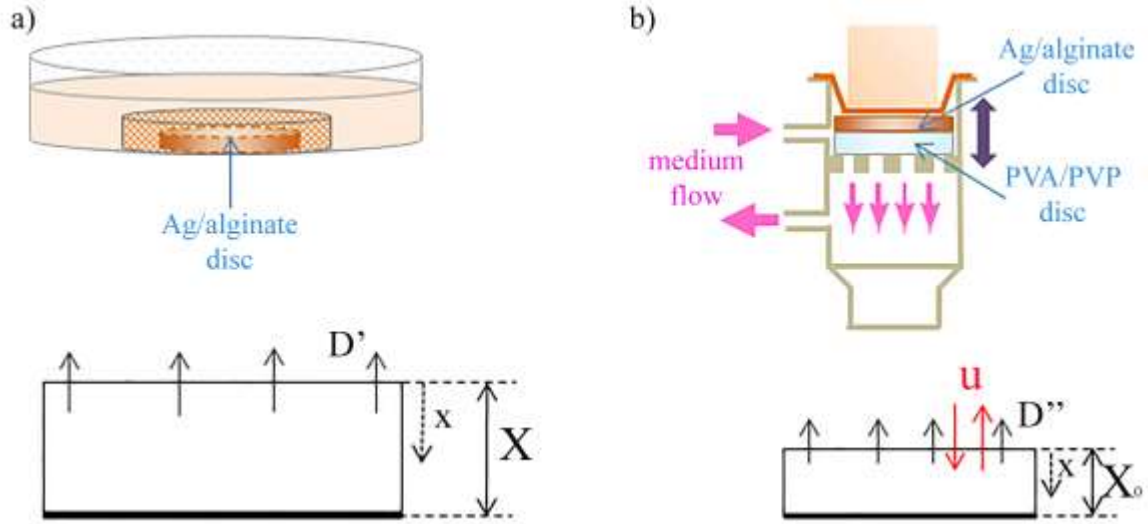

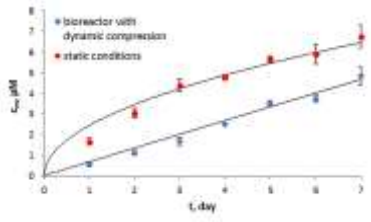


Table 1. Wavenumbers of the characteristic bands and corresponding assignments for Na-alginate solutions, Ca-alginate hydrogels, Ag/alginate colloid solutions and obtained Ag/alginate discs. Values were normalized regarding the ($CH_2$) bond, which was unchanged by electrochemical synthesis and gelling process.

| *Wavenumber, $cm^{-1}$* | | | | | | | | *Assignment* |
|---|---|---|---|---|---|---|---|---|
| *LG Na-alginate* | *HG Na-alginate* | *LG Ca-alginate* | *HG Ca-alginate* | *LG Colloid solution* | *HG Colloid solution* | *LG Disc* | *HG Disc* | |
| 3448 | 3444 | 3431 | 3435 | 3434 | 3446 | 3431 | 3416 | ν(OH) |
| 2929 | 2929 | 2929 | 2929 | 2929 | 2929 | 2929 | 2929 | $\nu_{as}(CH_2)$ |
| 1612 | 1612 | 1620 | 1640 | 1612 | 1619 | 1615 | 1618 | $\nu_{as}(COO^-)$ |
| 1421 | 1419 | 1428 | | 1418 | 1421 | 1428 | 1430 | $\nu_s(COO^-)$ |

Table 2. Compression moduli determined for different forms and compositions of Ca-alginate hydrogels reported in literature

| Hydrogelform, alginate composition | Loading rate, µm/s | Compression moduli, kPa | Ref |
|---|---|---|---|
| Discs, 1.7 % w/w Ag/alginate, M/G ratio 1.38 | 337.5 | 64.3 ± 3.3 | this work |
| Discs, 1.7 % w/w Ag/alginate, M/G ratio 1.94 | 337.5 | 43.7 ± 1.5 | this work |
| Disc, 1.5% w/w, M/G ratio 0.49 | 337.5 | 77.3 ± 1.1 | 14 |
| Disc, 2% w/w, M/G ratio 0.49 | 337.5 | 120.3 ± 2.8 | 14 |
| Disc, 2% w/w, M/G ratio 1.6 | 337.5 | 70.2 ± 3.9 | 14 |
| Disc ,1.5 % w/v, from *Laminariahyper borea* | 80 | 25 ± 0 | 70 |

| | | | |
|---|---|---|---|
| Disc, 2 % w/v, from *Macrocystis pyrifera* | 80 | 18 ± 2 | 70 |
| Disc, 1.5 % w/v, from *Durville apotatorum* (M/G ratio 2.1) | 100 | 3.8 ± 0.3 | 71 |
| Disc, 1.5 % w/v, from *Macrocystis pyrifera* (M/G ratio 1.43) | 100 | 11.5 ± 0.6 | 71 |
| Disc, 1.5 % w/v, from *Laminariahyper borea*(M/G ratio 0.49) | 100 | 32.7 ± 1.2 | 71 |
| Cylinder,2 % w/v, with G fraction of 0.68 | 200 | 105 ± 4.6 | 72 |
| Microbeads, 1.9 % w/v Ca/alginate | 337.5 | 141 ± 2 | 26 |
| Microbeads , 1.9 % w/v Ag/alginate | 337.5 | 154 ± 4 | 26 |